Lysis of Dysplastic but not Normal Oral Keratinocytes and Tissue-Engineered Epithelia with Conditionally Replicating Adenoviruses

Kamis Gaballah,[1] Allison Hills,[1] David Curiel,[3] Gunnel Hallden,[2] Paul Harrison,[4] and Max Partridge[1]

[1]Head and Neck Cancer Unit, King's College London, Guy's, King's and St. Thomas' Hospitals, and [2]Centre for Molecular Oncology, Institute of Cancer and the Cancer Research United Kingdom Clinical Centre, Barts and The London, Queen Mary's School of Medicine and Dentistry, London, United Kingdom; [3]Division of Human Gene Therapy, University of Alabama at Birmingham, Birmingham, Alabama; and [4]Beatson Institute for Cancer Research, Garscube Estate, Bearsden, Glasgow, United Kingdom

Abstract

There is no effective medical treatment for oral precancer, and surgery to remove these lesions is imprecise because abnormal mucosa extends beyond the visible lesion. Development of vectors for tumor-selective viral replication has been a significant advance, and viral lysis is well suited to destruction of oral precancerous mucosa. To facilitate evaluation of new treatments, we engineered dysplastic oral epithelium using keratinocytes isolated from dysplastic lesions. We show that these model systems recapitulate the key characteristics of the clinical lesions closely, and that topical delivery of the conditionally replicating adenovirus (CRAd) *dl922-947* can lyse tissue-engineered epithelia that show mild, moderate, or severe dysplasia, but normal oral epithelia are very resistant to this treatment. The lytic effect is determined by various factors, including the grade and proliferation index of the dysplastic epithelia. The presence of suprabasal cycling cells, expression of the coxsackie adenovirus receptor (CAR), the transcription cofactor p300, and other aberrations that affect the regulation of the cell cycle or apoptosis and promote viral replication may also be important. The ability of *dl922-947* to destroy engineered oral dysplasia was significantly greater than that observed using wild-type adenovirus, *d*/1520, or viruses modified to bypass cell entry dependent on the presence of CAR. Evidence of infection in clinical dysplastic lesions was also shown *ex vivo* using tissue explants. We conclude that *dl922-947* may provide an efficient molecular cytotoxic to dissolve oral dysplastic lesions. [Cancer Res 2007;67(15):7284–94]

Introduction

The results following treatment for oral cancer are disappointing because only half of all cases survive for 5 years after diagnosis. Locoregional recurrence is the most common cause of treatment failure, but a second tumor may also develop in a patch of precancerous mucosa. Surgery to remove these abnormal patches is unreliable because whereas some precursor lesions produce visible thickening or thinning of the mucosa, genetic aberrations extend well beyond the visible lesion, and there is no way of precisely defining where the margins of the lesions lie (1–5). There is no medical treatment that can effectively eliminate these precancerous patches, and innovative approaches that can prevent progression to malignancy are required.

Selectively replicating adenoviruses offer the potential to destroy precancerous lesions because they replicate in dividing cells. They are particularly useful for destroying lesions at accessible sites because they can be delivered topically and treatment can be repeated on multiple occasions. Several classes of conditionally replicating adenovirus (CRAd) have been developed to restrict viral replication to tumor cells by introducing modifications that abrogate viral functions that are essential for replication in normal cells but redundant in tumors. *dl922*-947 (6) and Δ24 (7) are examples of pRb-binding deficient CRAds with abrogated viral function based on deletions in E1A proteins. These abolish the binding of E1A to pRb family proteins, preventing release of the E2F transcription factor, activation of the adenovirus E2 promoter and cell cycle regulatory proteins that allow S-phase entry and replication in quiescent cells. These viruses can theoretically only replicate in cells where E2F is deregulated.

The coxsackie adenovirus receptor (CAR) is the primary receptor for adenoviruses, but internalization requires αv integrins. Because tumor cells frequently show reduced expression of these receptors (8–11), a second class of CRAds have been modified to bind to alternative receptors. Δ24RGD incorporates an Arg-Gly-Asp (RGD) sequence in the fiber that interacts with CAR and αv integrin (12), and Ad5/3Δ24 (13) uses the Ad3 receptors CD46 (14), CD80 (B7.1), and CD 86 (B7.2; ref. 15) for internalization.

The most extensively studied CRAd is d/1520 (ONYX 015) designed to selectively replicate and destroy p53-mutant cells (16). This virus carries an inactivating deletion encoding the E1B-55kD protein that inactivates p53 during viral replication, inhibiting p53-mediated apoptosis. Several tumor cell lines with intact p53 support replication of *d*/1520 and carry defects in p53-dependent pathways (17, 18). However, the oncolytic properties of this virus are attenuated due to the presence of the E1B deletion. In a pioneering report, Rudin et al. (19) showed that daily application of *d*/1520 as a mouthrinse could reduce the severity of oral dysplastic lesions, providing initial evidence that CRAds can penetrate dysplastic epithelia. Efficient replication of CRAds and evidence of viral lysis have been observed maintaining tumor explants *ex vivo* (20). However, normal tissues and dysplastic lesions may rapidly undergo autolysis, and we were unable to conclusively show viral replication using tissue explants. Recognizing these limitations, we developed a new three-dimensional culture system maintaining oral keratinocytes derived from dysplastic lesions on fibroblast-containing collagen gels. The

Requests for reprints: Max Partridge, Head and Neck Cancer Unit, King's College London, Guy's, King's and St. Thomas' Hospitals, Guy's Tower, St. Thomas Street, London SE1 9RT, United Kingdom. Phone: 44-207-346-3474; Fax: 44-207-346-3753; E-mail: oralsurgery@partridgekcl.co.uk.

doi:10.1158/0008-5472.CAN-06-3834

phenotypic characteristics of the engineered dysplastic and oral epithelia were compared with normal and lesional oral mucosa to show that they recapitulate the tissue morphology closely. These model systems were used to study the response of oral keratinocytes to wild-type adenovirus, *dl*922-947, Δ24, *d*/1520, Δ24RGD, and Ad5/3Δ24. We show that the ability of *dl*922-947 to dissolve dysplastic and malignant oral epithelia was superior to the other modified viruses, and that this treatment had minimal toxicity in normal oral epithelia.

Materials and Methods

Tissues. The study was approved by the Ethics Committee of King's College Hospital. Informed consent was obtained from all patients. Samples of normal oral mucosa were obtained from non-, para-, and fully keratinized sites. Lesional mucosa was obtained from portions of biopsy material that were not selected by the pathologist for light microscopy.

Monolayer culture. Normal oral keratinocytes (NOK) were grown from tissue explants and maintained with a J2 fibroblast feeder layer (21). Established cultures of oral keratinocytes derived from lesions showing moderate/severe dysplasia D6 (22), mild/moderate dysplasia DOK (23), moderate dysplasia D20 (22), and moderate/severe dysplasia POE9n (24) were also grown with a J2 feeder layer. Four new strains of dysplastic oral keratinocytes were evaluated. LDOK was established from a severe dysplasia on the lingual alveolus. This strain carries a p53 gene mutation (G-T at codon 248) and does not express p16. CDOK was established from a mild dysplasia at the commissure, LTDOK was established from a mild dysplasia on the lateral tongue, and SPDOK from a moderate dysplasia on the soft palate. These strains and D6 are all mortal, wild type for p53, and express p16. D20, DOK, and POE9n carry a *p53* gene mutation and do not express p16 (21–23); D20, DOK, and LDOK are immortal, and POE9n has an extended culture life span. The JHU022 (8), HN5 (25), and CAL 27 [CRL-2094, American Type Culture Collection (ATCC)] squamous carcinoma cell lines were maintained in DMEM, Hams-F12, and 10% fetal bovine serum (Invitrogen).

Preparation of engineered oral epithelia. Keratinocytes (1×10^6) derived from normal oral epithelia (p2) and dysplastic lesions (p2-18) were grown on collagen gels and raised to the air-medium interface on day 2 (26). In some experiments, keratinocyte growth factor (KGF; Invitrogen) was substituted for epidermal growth factor (EGF). The grade of dysplasia was established for each epithelium by considering the changes in architecture and cytologic features.

Recombinant adenoviruses. We evaluated *dl922-947*, Δ24, d/1520, Δ24RGD, and Ad5/3Δ24. Δ24 and *dl922-947* are similar viruses with deletions at 923 to 946 and 922 to 947 bp, respectively. AdGFP is E1 deficient and carries the gene for green fluorescent protein (GFP) under control of the cytomegalovirus promoter; *dl*312 has a total E1A gene deletion. These viruses and Adwt were propagated on 293 cells and purified using cesium chloride density gradient centrifugation.

Cytotoxicity assays. The cytotoxicity of the viruses was established by MTS assay. Keratinocytes were plated at 1×10^4 with a J2 feeder layer and after 24 h were either mock infected or infected with a range of viral particles (vp) for 90 min in serum-free media (SFM). After 7 days, MTS solution (Promega) was added, and the absorbance was measured at 490 nm. The keratinocytes were also grown to 40% confluence before infection with 1, 10, or 100 vp per cell for 90 min, and the cytopathic effect was examined by staining with crystal violet after 7 days.

Viral infection of tissue explants. Explants were prepared from clinical dysplastic lesions ($n = 10$) and normal oral mucosa ($n = 10$) and exposed to 10^9 vp of *dl922-947*, Adwt or *d*/312 in SFM, adding the virus to the uppermost layer as previously described (20). After 10, 20, 30, or 40 h, the explants were snap frozen in liquid nitrogen.

Viral infection of tissue-engineered oral epithelia with keratinocytes from normal tissues and dysplastic lesions. Seven days after raising the engineered epithelia, the cultures were either mock infected or infected with 1, 10, or 100 vp per cell, adding the virus to the uppermost layer in SFM for 2 h. After 7 to 14 days, each culture was divided into two. One-half was snap frozen in liquid nitrogen; the other was fixed in formalin. Cytopathic effect and general tissue morphology was evaluated by examining step-serial paraffin or frozen sections by two observers blinded with respect to the treatment group and time point.

Viral replication assays. Keratinocytes grown in monolayer or tissue-engineered epithelia were collected together with the medium and virus released by three freeze-thaw cycles quantified with the TCID 50 assay using 293 cells and the AdenoX Rapid Titer kit (Clonetch).

Immunohistology. Expression of CAR was with clone CRL-2379 (1:1,000, ATCC) and the polyclonal antibody CAR 72 (1:1,000; ref. 27). The EGF receptor was detected with GRO1L (1:40; Oncogene Science, DAKO), E cadherin with BTA1 (1:200; R&D Systems), CD44 v6 with VFF-7 and v7 with VVF-9 (1:50–1:200; Abcam), occludin with the polyclonal antibody (1:100; Zymed, Invitrogen), laminin 5 with D4B5 (1:200; Chemicon Chandlers Ford), collagen 4 with C1V22 (1:50; DAKO), fibronectin with IST-9 (1:200; Abcam), p16 with F-12 (1:50; Santa Cruz, Autogen Bioclear), αvβ3 with clone 1976 and αvβ1 with clone 1976 (1:50; Chemicon), and filaggrin with BT-576 (Biogenesis). Immunolocalization of cytokeratins 10, 13, and 19 was with 9025, BA16, and 1384-500, respectively (all 1 in 50; all Abcam). p300 was detected with MS-586-NM1 (1:20; Lab Vision) and Ki67 with M7240 (1:50; DAKO). Sections stained with monoclonal antibodies were incubated with biotin-conjugated rabbit anti-mouse antibody followed by streptavidin-horseradish peroxide complex (DAKO). The Ki67 proliferation index was determined for the basal and suprabasal compartments of the epithelium as the mean percentage of positive cells ±SE in five contiguous fields at 100× magnification. Immunoreactive cells were counted using Qwin image analysis software. A similar protocol was followed when assessing the proliferation index for monolayers, analyzing five fields captured at random at 100×.

Viral early gene expression was detected with anti-E1A (1:50; Oncogene Science) and quantitated by counting the number of cells that were strongly positive as E1A "spots" for five fields at 100×. Viral hexon protein was detected with anti-Ad5 antiserum (1:200; Cocalico Biologicals).

Fluorescence-activated cell sorting analysis and Western blotting. Cell cycle analysis was done 48 h following infection of the keratinocytes with 10 vp per cell. Lysates were resolved by PAGE, and membranes were probed with antibodies for p16, Rb, RbP, cyclin D1, cyclin E, cdk4, and cdk6 (1:1,000, clones 554079, 554136, 9308, 554180, 559693, 554086, 554182; all BD PharMingen, Abcam).

Statistical analysis. Statistical analyses were done using SPSS. A descriptive analysis was done initially followed by one-way ANOVA. Comparison of the lysis scores was with StatXact3 for Windows using Xact nonparametric inference to allow for small sample size.

Results

Characterization of the G_1-S checkpoint for dysplastic oral keratinocytes. We investigated the expression of key cell cycle proteins for the normal, dysplastic, and malignant keratinocytes. We found an increase in the levels of RbP in the immortal dysplastic keratinocytes, the JHU022 cell line and for the POE9n strain (Fig. 1*A*). Higher levels of hypophosphorylated Rb were present in D6 and NOK. p16 was expressed by all mortal dysplastic keratinocytes, but was absent from POE9n, D20, DOK, and LDOK. Immunohistology confirmed the expression of p16 by D6, SPDOK, CDOK, and LTDOK. The immortal dysplastic strains showed increased expression of cyclin D1, but levels of the cdks were consistent for all cell types.

Lysis of dysplastic and malignant but not NOKs after infection with *dl*922-947 or Δ24 in monolayer. Oral keratinocytes derived from normal and dysplastic lesions were infected with *dl*922-947, Δ24, Adwt, and *d*/1520 to assess the cytopathic effect, (Fig. 1*B*). The MTS assay showed that lysis was most effective for the malignant and dysplastic keratinocytes, with the

percentage of viable cells after infection with 10 vp per cell of *dl*922-947 in the range 20% (JHU022) to 68% (POE9n), with an average of 43% for the five strains of dysplastic keratinocytes overall. When these strains were infected with 1,000 vp per cell of *dl*922-947, the average percentage of viable cells was 33%. In contrast, NOK were very resistant to lysis, with *dl*922-947 at 10 vp per cell and 87% viable cells remained, but they were readily lysed by Adwt (42% viable cells, $P < 0.005$). The efficiency of the lytic response was compared for the D6, POE9n, and D20 dysplastic oral keratinocytes, selected as examples of strains with a finite, extended, and immortal phenotype, by estimating the amount of *dl*922-947 required to produce 40% lysis. This comparison showed that the D6 strain lysed most readily followed by D20, but that the POE9n stain did not reach this threshold even after exposure to 1,000 vp per cell.

The D20, DOK, and POE9n strains, together with NOK, were also exposed to *d*/1520. This CRAd produced only limited lysis in comparison to the effect of *dl*922-947, and after exposure to 10,000 vp per cell, 88%, 72%, and 96% viable cells remained, respectively, but NOK were more readily lysed by this virus (72% viable cells after exposure to 1,000 vp per cell). The HN5 tumor cell line also showed lysis with *d*/1520 after exposure to 10,000 vp per cell (<60% viable cells remained). Crystal violet staining confirmed efficient lysis of the dysplastic strains with *dl*922-947 and resistance to *d*/1520 (data not shown).

Infection with *dl*922-947 or Δ24 induces S phase in dysplastic but not NOKs. Infection of the D6, POE9n, and D20 strains with 10 vp of *dl*922-947 induced a 3.3-, 2-, and 4-fold increase, respectively, in the number of cells in S phase when compared with the E1-deleted CRAd, *dl*312 ($P < 0.05$), but the number of cycling normal keratinocytes was not changed significantly. As anticipated, Adwt induced a significant increase in the number of cycling cells for all strains (Fig. 1*C*). Induction of S phase in dysplastic oral keratinocytes was confirmed by an increase in the proliferation index following infection with 10 vp per cell of *dl*922-947 or Adwt for all strains. Representative examples are shown for CDOK and NOK (Fig. 1*D*), together with the pattern of expression of Ki67 and E1A.

Infectivity of normal and dysplastic oral epithelium *ex vivo*. Explants of normal and dysplastic oral epithelium showed varying degrees of autolysis within a few hours, and some had disintegrated by 24 h, although the basal keratinocytes were often retained. Expression of hexon and E1A was detected in some cells at the edges of 4 of 10 explants of dysplastic tissue 30 h after infection with *dl922-947*, or Adwt (Fig. 2*A*), but extensive autolysis precluded further experimentation.

Morphologic and phenotypic characterization of tissue-engineered oral epithelia. Morphologic assessment of the epithelia generated *in vitro* using keratinocytes derived from nonkeratinized sites showed a multilayered epithelium resembling the parent tissue with a polarized basal layer and larger spinous cells (Fig. 2*B*). For keratinized epithelia, the upper cells became flattened as keratohyaline granules accumulated. Rete ridges were rarely observed, but normal differentiation was confirmed by suprabasal expression of keratin 13 for nonkeratinized oral epithelia (>60% positive cells) and keratin 10 (20–40% positive cells) for keratinized epithelia. The patterns of expression of the EGF receptor, CD44, E cadherin, and occludin were as obtained for normal oral mucosa. The rate of proliferation of the nonkeratinized oral epithelia was greater than for keratinized tissue, mimicking the pattern observed *in vivo* (28).

Maintaining the dysplastic keratinocytes with EGF, as opposed to KGF, supported the development of epithelia where the severity of the dysplasia was similar to that reported for the parent lesion. These epithelia showed architectural and cytologic disturbances that were scored as either mild (DOK, SPDOK), moderate (D6, CDOK), moderate to severe (POE9n, D20) mirroring the changes found in the *in vivo* dysplasias (Fig. 2*A*). Dysplastic keratinocytes isolated from two lesions yielded tissue-engineered epithelia with a phenotype that was graded as more severe than the parent tissue (LTDOK-clinical lesion moderate dysplasia, engineered epithelia severe dysplasia; LDOK-clinical lesion severe dysplasia, engineered epithelia carcinoma *in situ*). The basal layer was frequently not polarized, and suprabasal mitoses were observed in the dysplastic epithelia generated with the D6, POE9n, D20, and LDOK strains. The Ki67 proliferation index for the epithelia generated with mortal dysplastic strains (p2-4) was lower than anticipated when compared with NOK, but epithelia derived using the immortal dysplastic strains showed higher rates of proliferation and frequent suprabasal mitoses, mimicking the *in vivo* scenario.

The pattern of keratinization was variable with dysplastic keratinocytes with a finite life span generating thin, highly keratinized epithelia, whereas the immortal strains produced cultures that were thicker and less well keratinized. Cytokeratin 13 was expressed in the suprabasal layers of the tissue-engineered epithelia prepared with D6, CDOK, LTDOK, and SPDOK (40–60% positive cells), DOK (>60% positive), D20 and POE9n (20–40% positive), LDOK (<20% positive) and in the basal layer for JHU022. Cytokeratin 10 was expressed by the DOK and D20 epithelia (20–40% positive). No drop-shaped rete pegs were observed, and the engineered epithelia lacked the hyperplasia and excessive surface keratinization that may be a feature of clinical lesions. The engineered dysplastic epithelia expressed the EGF receptor and E cadherin on more cell layers than found for the matched normal tissue, mimicking the findings for *in vivo* dysplastic lesions. Further detailed characterization of expression of keratin 19, filaggrin, fibronectin, CD44, occludin, collagen 4, and laminin 5 showed patterns characteristic for a range of clinical lesions showing mild ($n = 12$), moderate ($n = 8$), or severe ($n = 6$) dysplasia (data not shown). The $\alpha v\beta 3$ and $\alpha v\beta 1$ integrins were detected in the basal and lower spinous cells of normal oral mucosa and dysplastic lesions, but the engineered dysplastic epithelia showed only low (D20 and DOK) or no expression (POE9n) of these subunits. However, these integrins were visualized at the cell membranes for the engineered D6 and DOK epithelia. The staining also seemed to be intracellular and to diffuse into the collagen gel. Comparison of the immunophenotypic profile for the DOEs with the matched clinical lesion (CDOK, SPDOK, LTDOK) showed increased expression of keratin 13 for the engineered tissue equivalents (on average, 15% more positive cells) and a reduced Ki67 index (data not shown) when compared with the matched clinical lesion, but all other markers were similar. These phenotypic changes were consistent for epithelia generated with the immortal keratinocytes maintained through serial passage. The JHU022 cell line generated an epithelium that resembled noninvasive carcinoma *in situ* (data not shown).

Infection of tissue-engineered oral epithelia with AdGFP. When the engineered normal oral epithelia were infected with AdGFP, expression of GFP was found only after infection with 100 vp per cell and limited to the uppermost cell layers (Fig. 2*B*). This indicates that the virus is able to gain entry into the superficial cells due to disruption of tight junctions as each differentiating layer is lost, but it is unable infect the deeper layers. When

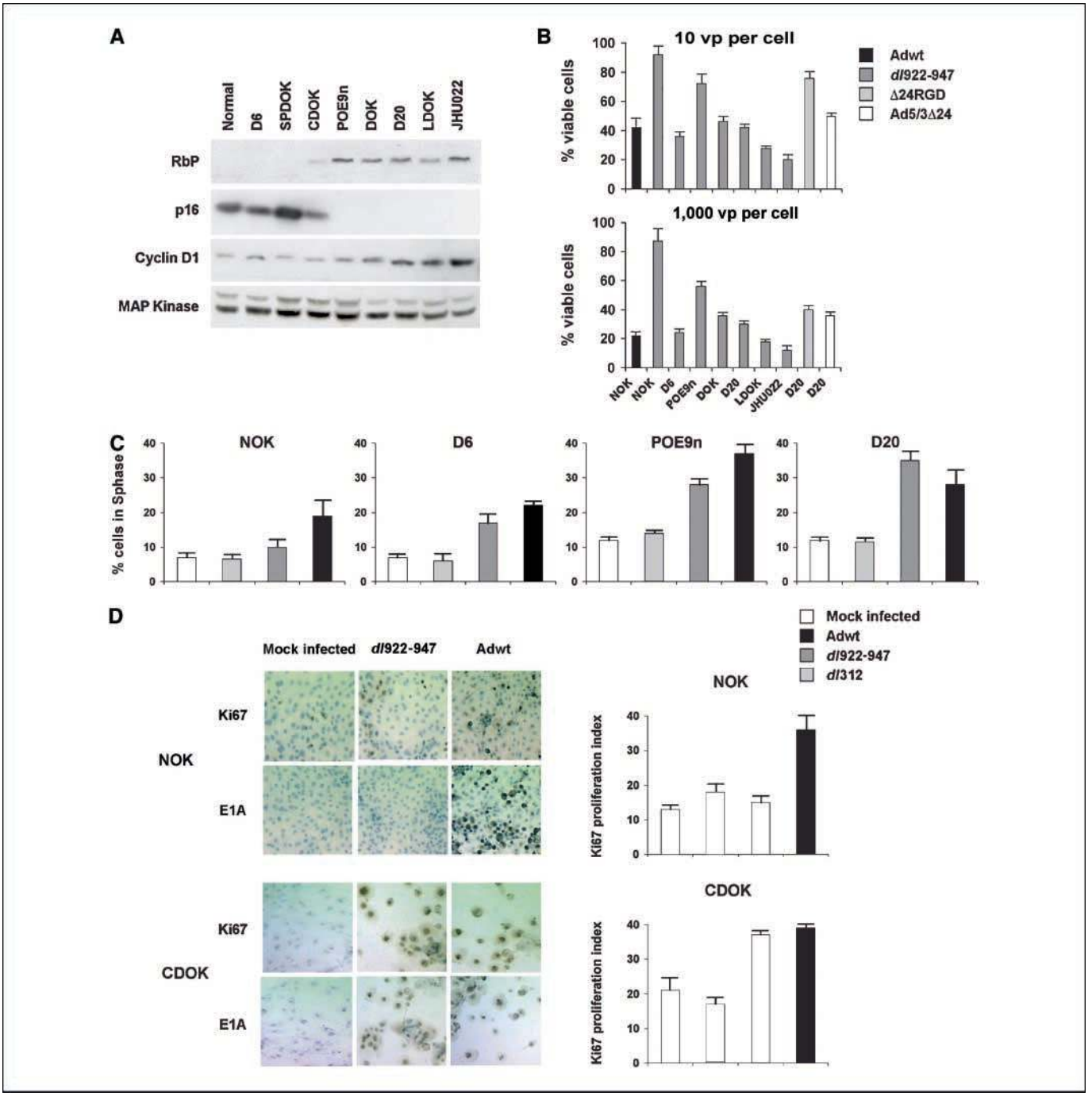

Figure 1. Characterization of dysplastic oral keratinocytes and demonstration of the lytic effect of CRAds for oral dysplasia in monolayer culture. *A,* levels of RbP, p16, and cyclin D1 in normal (NOK), dysplastic (*D6, SPDOK, CDOK, POE9n, DOK, D20, LDOK*), and malignant (*JHU022*) oral keratinocytes. The expression of the proteins was measured by Western blotting using mitogen-activated protein kinase as a loading control. *B,* cell death induced by Adwt, *dl*922-947, d/1520, Δ24RGD, and Ad5/3Δ24 in normal and dysplastic oral keratinocytes after infection with 10 vp per cell and 1,000 vp per cell. The D6 strain showed most lysis following infection with *dl*922-947, and Ad5/3Δ24 is more lytic than Δ24RGD at 10 vp per cell. NOKs showed more lysis that the D20 dysplastic strain when exposed to d/1520 at 1,000 vp per cell. *C,* induction of S phase following infection of NOK, D6, POE9n, and D20 with 10 vp per cell of *dl*312, *dl*922-947, d/1250, or Adwt (see key below). Exposure to *dl*922-947 and Adwt increased the proportion of dysplastic oral keratinocytes in S-phase, but the normal cells only showed S phase induction after exposure to Adwt. *D,* the increased Ki67 proliferative index for NOKs and the CDOK dysplastic strain following exposure to Adwt and for the CDOK strain after exposure to *dl*922-947. The pattern of positive Ki67 and E1A staining following exposure of the CDOK strain to *dl*922-947 confirmed that this CRAd induced S-phase in dysplastic but not normal keratinocytes.

the dysplastic counterparts were infected with this virus, the pattern was as described for the normal epithelia, although the LDOK strain expressed GFP in the spinous layer at sites where loss of cohesion was apparent (Fig. 2*B*).

Tissue-engineered normal oral epithelia are very resistant to lysis by *dl*922-947 or Δ24. Infection of tissue-engineered normal oral epithelia derived from 9 of 12 strains of oral keratinocytes from nonkeratinized sites with *dl*922-947 or Δ24

produced an increase in keratinization but no evidence of lysis. Two strains showed very limited lysis and a single stain of buccal keratinocytes foci of ballooning degeneration with loss of cells from the tissue, but the surface layers were retained intact. Similarly, very limited lysis was observed for 2 of 19 samples of engineered epithelia derived from para- or fully keratinized normal oral mucosa following exposure to *dl*922-947 or Δ24. In contrast, infection with Adwt induced more lysis in all engineered normal epithelia (Fig. 2*B*).

Efficient lysis of tissue-engineered oral dysplastic epithelia following infection with *dl*922-947 or Δ24. The lytic effect of *dl*922-947 and Δ24 was dose dependent for all engineered oral dysplasias evaluated, and the lysis score was significantly higher when epithelia prepared with the dysplastic and normal strains were compared following exposure to 100 vp per cell ($P = 0.0222$, Table 1). A reverse effect was found after infection with Adwt ($P = 0.0222$). Cytopathic changes included an increase in the level of superficial keratinization, the presence of bursting cells, ghost cells, and superficial debris. These changes seemed more rapid in the spinous and basal layers as the number of vp was increased. Examples of the patterns of lysis are shown for the D20, DOK, POE9n, and D6 strains (Fig. 3*A*). Efficient dissolution of the D20 and DOK epithelia after exposure to 100 vp per cell is shown at days 7 and 12, respectively. As the lytic foci coalesced, cavities filled with fluid and floating cells were often detected, and gross disturbances in the tissue architecture and marked cytologic changes were apparent as the tissue dissolved. The pattern of lysis of the POE9n and D6 epithelia, after exposure to 100 vp per cell, is also shown (Fig. 3*A*) The LDOK epithelia also showed very efficient lysis with complete loss of all dysplastic keratinocytes by day 7. Infection of these epithelia with Adwt produced a more limited response (Table 1), although occasional foci of more extensive lysis were observed (Fig. 2, *bottom, right*).

The pattern of expression of the viral hexon protein showed that *dl*922-947 or Δ24 reached the deeper layers of the dysplastic epithelia after exposure to 10 vp per cell for the D20 and LDOK strains that lysed most efficiently (Fig. 3*B*). Expression of hexon protein also increased as viral replication and lysis occurred. Dysplastic epithelia with a lower lysis score, for example, that derived from the POE9n strain, showed a more heterogeneous pattern of staining.

Evidence of replication of *dl*922-947 or Δ24 in tissue-engineered oral epithelia. Evidence of viral infection after exposure to *dl*922-947 was confirmed by expression of E1A with the highest number of E1A spots counted for the malignant and immortal dysplastic epithelia (Figs. 3*C* and 4*A*). The mortal strains showed expression of E1A despite having a low Ki67 proliferative index. Evidence of replication of *dl*922-947 and Adwt was shown for all infected dysplastic epithelia with the highest number of infectious units detected for the strains showing the most lysis (Fig. 4*B*).

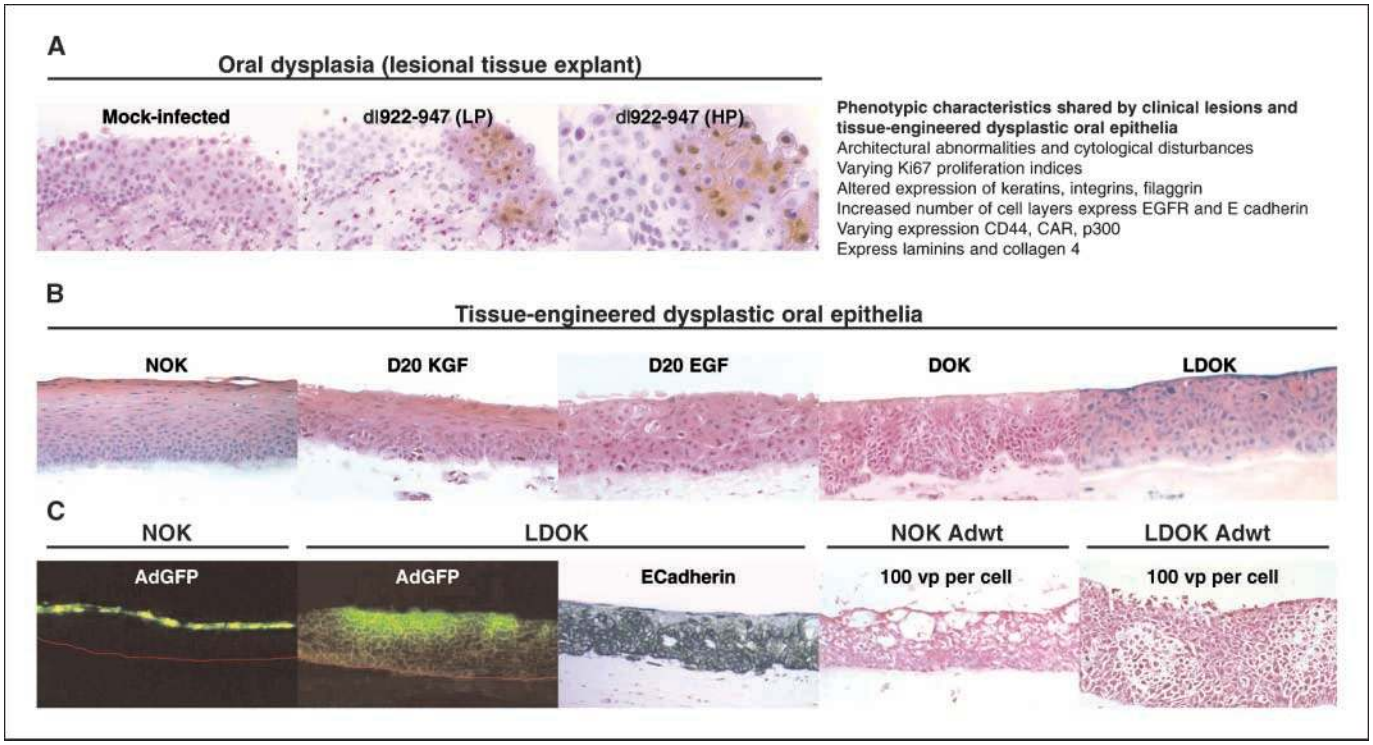

Figure 2. Dysplastic oral epithelia infected with *dl*922-947, summary of the phenotypic similarities of dysplastic oral lesions and tissue-engineered dysplastic oral epithelia, morphologic characteristics of representative engineered normal and dysplastic epithelia and the lytic effect of Adwt. *A,* oral dysplastic tissue infected with *dl*922-947 to determine the infectivity of clinical lesions by staining for intranuclear expression of E1A as an indication of viral replication 30 h postinfection in culture, together with the mock-infected control at low and high power (*LP, HP*). These tissues also show evidence of autolysis. *B,* H&E-stained sections of normal (*NOK*) and representative examples of tissue-engineered dysplastic oral epithelia, including those prepared from the D20 strain maintained with KGF (mild dysplasia), D20 maintained with EGF (severe dysplasia), DOK (mild dysplasia), and LDOK (carcinoma *in situ*). *C,* transduction with AdGFP showed that expression of this marker protein was limited to the superficial layer for engineered normal oral epithelia and to focal areas of the upper and middle layers of the engineered LDOK dysplastic epithelia. The pattern of expression of E cadherin is also shown for this epithelium. The lytic effect of Adwt was greater for tissue-engineered oral epithelia prepared using NOK after exposure to this virus at 100 vp per cell for 14 d when compared with the engineered dysplastic oral epithelia, although occasional foci of more extensive lysis were detected as typified by the response of the LDOK strain.

Table 1. Comparison of the lytic effect of *dl*922-947, Δ24RGD, Ad5/3 and Adwt at 1, 10, and 100 vp per cell for normal, dysplastic, and malignant engineered oral epithelia 14 d after infection

Cell type	*dl*922-947			Δ24RGD			Ad5/3			Adwt	Ki67 proliferation index	
	1	10	100	1	10	100	1	10	100	100	Basal	Suprabasal
NK	1	1	1	0	1	1	1	1	1	3	47.12 ± 2.25	5.67 ± 1.45
K	1	1	1	0	0	1	0	1	1	3	35.96 ± 1.45	7.09 ± 1.91
SPDOK	1	2	3	0	1	1	1	1	2	2	2.01 ± 0.01	1.0 ± 0.1
LTDOK	1	2	3	0	1	1	1	1	2	2	2.26 ± 0.1	1.0 ± 0.1
CDOK	1	2	4	1	1	2	1	2	2	2	32.02 ± 3.11	11.4 ± 2.37
D6	1	2	4	0	1	3	1	1	3	2	2.1 ± 0.01	1.23 ± 0.15
D20/KGF	1	2	3	0	1	1	1	1	2	2	76.02 ± 1.08	9.77 ± 0.44
D20/EGF	1	3	4	0	1	2	1	1	3	2	59.74 ± 4.00	13.98 ± 1.38
POE9n	1	2	3	0	1	2	1	1	3	2	54.49 ± 4.08	17.88 ± 1.91
DOK	1	2	4	2	2	3	1	1	3	2	80.36 ± 0.93	4.59 ± 0.96
LDOK	2	3	5	1	1	2	2	2	4	2	74.7 ± 3.48	66.01 ± 5.32
JHU022	3	4	5	1	1	2	2	2	4	2	79.20 ± 1.98	82.23 ± 1.12

NOTE: The Ki67 proliferative index is also shown for the tissue equivalents generated using these strains (NK, normal nonkeratinizing mucosa; K, normal keratinizing mucosa). Visual scoring for CRAd infection: 1, occasional lytic cavities in the upper epithelium and some loss of polarity of the basal cells at day 14; score 2, areas of lysis in the upper layers extending to the spinous cells by day 14; score 3, lytic cavities in the upper epithelium with a mixed pattern of lysis in the lower layers with areas where all cells were lost mixed with foci where the basal cells remained at day 14; score 4, many lytic cavities throughout the epithelia at day 7 and complete lysis by day 14; score 5, complete lysis of the epithelium by day 7.

Phenotypic characteristics of the tissue-engineered dysplastic oral epithelia modulate the severity of lysis with *dl*922-947. The lysis score was not related to the severity of dysplasia in that following infection with *dl*922-947 at 100 vp per cell, epithelia derived from the JHU022 and LDOK strains dissolved as completely as the epithelia derived using the D6, D20 (maintained with EGF), and the DOK strains. However, the engineered dysplastic epithelia derived from LTDOK, POE9n, D20 (maintained with KGF), and SPDOK showed a mixed pattern of complete and partial lysis at the same dose level.

The tissue-engineered dysplastic oral epithelia were characterized by different proliferation indices and patterns of Ki67 expression (Table 1, Fig. 5*A*). In general, the dysplastic epithelia with the highest rate of basal and suprabasal proliferation showed the most efficient lysis after exposure to *dl*922-947. When the D20 epithelia was maintained with EGF, as opposed to KGF, more suprabasal mitoses were detected (Table 1), and after exposure to *dl*922-947 or Δ24, the lysis score (Table 1) and number of E1A spots was increased (Fig. 4*A*), supporting the view that the number of cycling suprabasal cells modulates the lytic response. However, this is not the only factor influencing the extent of lysis because some basal cells remained when the POE9n epithelia, which shows frequent suprabasal mitoses, was infected with *dl*922-947. The D6 engineered oral epithelia, with a low Ki67 proliferative index, also lysed completely (Table 1).

Our detailed survey of patient-derived normal oral mucosa revealed that CAR was detected at cell membranes throughout the epithelium at nonkeratinized sites, and that expression of this receptor was reduced on the upper differentiating cells at keratinized sites. Most engineered dysplastic oral epithelia showed strong membranous and or weak cytoplasmic staining for CAR on the basal and middle cell layers, and there were many areas where the superficial cells expressed this receptor, (Fig. 5*B*). The POE9n epithelia and 4 of 16 clinical dysplastic lesions showed areas where there was almost no CAR on the basal cells, although immunoreactive cells were found at higher levels and for other patches of basal cells at different sites along the basement membrane (Fig. 5*B*). The D20 and DOK epithelia showed only low levels of expression of αv integrin, yet supported lytic viral replication and lysis.

We examined the pattern of expression of p300, a transcription factor that can initiate DNA synthesis and facilitate viral and cellular DNA replication (24) because these viruses retain the sequences that bind to this cofactor. We found that p300 was restricted to the basal cells of nonkeratinized tissues but detected throughout the epithelia *in vivo* and *in vitro* at keratinized sites (Fig. 5*C*). The mortal engineered dysplasias expressed this cofactor throughout the tissue (Fig. 5*C*), whereas those generated with the immortal stains, and the clinical dysplastic (Fig. 5*C*) and malignant lesions, showed a more variable pattern, with some cultures and tissues showing strong staining for this cofactor, whereas others had a more focal pattern.

Δ24RGD and Ad5/3Δ24 modified to enter epithelial cells via different receptors do not lyse tissue-engineered oral dysplasia efficiently. The cytotoxicity of Δ24RGD and Ad5/3Δ24 for normal and most dysplastic oral keratinocytes, maintained as monolayers, was less than for *dl*922-947. The D20 strain was most sensitive to these viruses, but the 40% cell-killing threshold was only reached following infection with 1,000 vp per cell of Ad5/3Δ24 or Δ24RGD (Fig. 1*B*).

The engineered dysplasias showed less lysis when the effects of exposure to Δ24RGD or Ad5/3Δ24 were compared with *dl*922-947 (Table 1). There was no relationship between expression of αv integrins and lysis after exposure to Δ24RGD, although hexon and E1A were frequently detected in the upper and spinous layers, suggesting that these CRAds are able to infect dysplastic keratinocytes, but that their ability to replicate may be impaired when compared with *dl*922-947.

The POE9n dysplastic epithelium was also infected with *dl*922-947 followed by exposure to Ad5/3Δ24 or Δ24RGD. The basal cells of this epithelia do not express CAR or significant levels of αv integrins, but a second round of infection with a CAR-independent vector increased the number of sites where lysis of basal cells occurred when compared with a single round of infection with *dl*922-947 (data not shown).

Discussion

We report that topical delivery of *dl*922-947 can dissolve tissue-engineered oral dysplasia, and that the normal counterparts are very resistant to lysis. The lytic effect of *dl*922-947 for oral dysplasia was significantly greater than that observed with *d*/1520 or CRAds modified to bind to alternative cellular receptors. Previous studies have shown that *dl*922-947 and Adwt can infect and replicate in

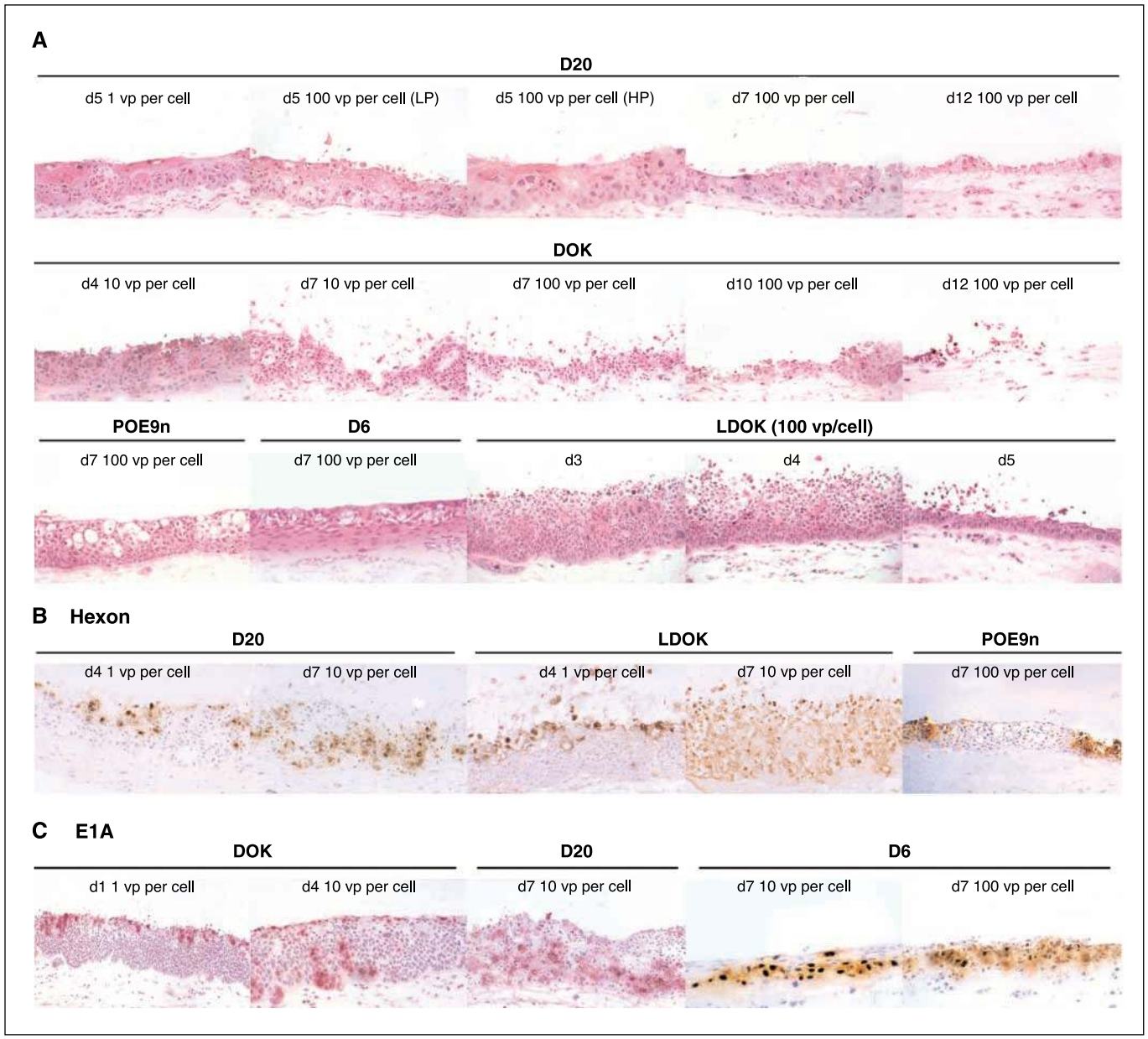

Figure 3. Lytic effect of *dl*922-947 and expression of viral hexon protein and E1A indicating that this CRAd is able to reach the deeper layers of the epithelium, replicate, and cause lysis in a dose-dependent manner. *A, top row,* destruction of the tissue-engineered D20 dysplastic epithelium after exposure to 1 and 100 vp per cell of *dl*922-947 showing superficial keratosis and the appearance of lytic cavities at day 5 at low and high power (*LP, HP*). The number of ghost cells and superficial debris increased over time such that there is significant thinning of the epithelium at day 12 and loss of all keratinocytes by day 14. *Second row,* similar treatment effects after exposure of the engineered DOK dysplastic epithelium to 10 and 100 vp per cell. *Third row,* lytic cavities developing for the tissue-engineered POE9n and D6 dysplastic epithelia after exposure to 100 vp per cell. Rapid lysis of the engineered LDOK epithelium is also shown. *B,* representative tissue-engineered dysplastic oral epithelia showing expression of hexon for the D20 and LDOK strains at day 4 following infection with 1 and 10 vp per cell of *dl*922-947, respectively. As the dose of virus is increased, hexon protein is detected in the lower epithelial layers. Infection of the engineered LDOK epithelia with 10 vp per cell produced complete dissolution, and increased expression of hexon protein is shown at days 1 and 7 as viral replication and lysis progressed. In contrast, the POE9n dysplastic epithelium showed a focal pattern of hexon expression at day 7 following exposure to 100 vp per cell *dl*922-947. *C,* expression of E1A was dose dependent, and examples are shown at days 1 and 4 for the engineered LDOK epithelia after infection with 1 and 10 vp per cell of *dl*922-947, for the D20 dysplastic epithelium at day 7 after exposure to 10 vp per cell, and for engineered D6 epithelia at day 7 after exposure to 10 and 100 vp per cell.

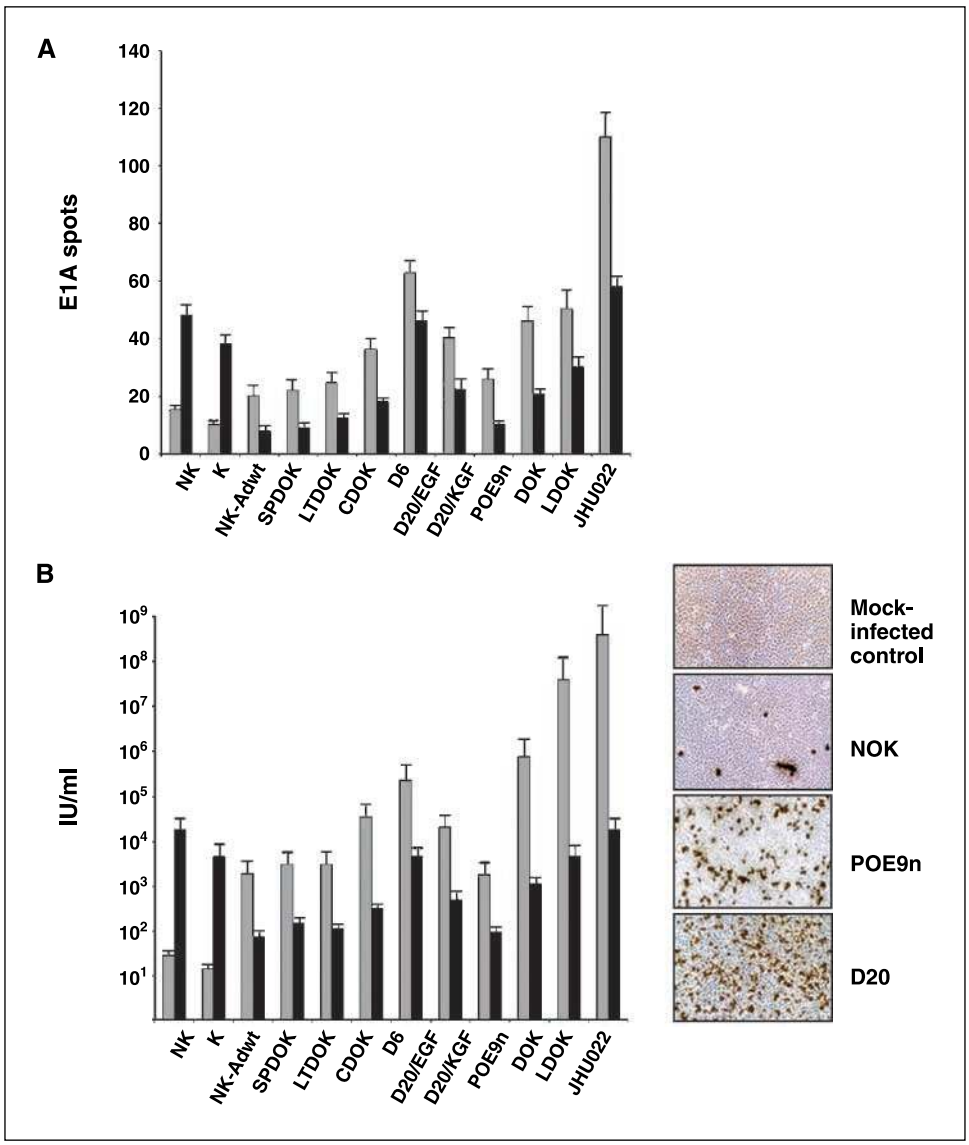

Figure 4. CRAds replicate in dysplastic oral keratinocytes. *A,* demonstration of viral replication by counting E1A spots following infection of the tissue-engineered epithelia prepared with normal (*NK*, nonkeratinized, *K*, keratinized), dysplastic, and malignant oral keratinocytes with 10 vp per cell *dl*922-947 and with Adwt. The scores are shown for the normal epithelia that showed evidence of infection with *dl*922-947. *B, left, de novo* production of *dl*922-947 and Adwt following infection and lysis of normal, dysplastic, and malignant tissue engineered oral epithelia 6 to 12 d after infection. The results are presented as mean infectious units (*IU*) per milliliter ±SE. *Right*, detection of hexon protein with the AdenoX Rapid Titer kit for freeze-thaw derived lysates from mock-infected 293 cells and engineered epithelia generated with NOKs and the POE9n and D20 strains of dysplastic keratinocytes.

clinical lesions after 48 h (20), but explants of normal and dysplastic oral mucosa underwent rapid autolysis, and we were only rarely able to maintain these tissues over this time frame. Recognizing these limitations, we developed an *in vitro* system to tissue engineer normal and dysplastic epithelia showing mild, moderate, and severe dysplasia using keratinocytes derived from normal tissues and clinical lesions. These tissue equivalents showed different rates of proliferation, subrabasal mitoses, disordered keratin expression, and increased expression of the EGF receptor and E cadherin when compared with normal tissues, mimicking the *in vivo* situation. The engineered epithelia are comprised of different numbers of viable cell layers, but lack rete ridges that are a feature of clinical lesions. The immortal dysplastic oral epithelia and the normal counterparts also showed a modest increase in the Ki67 proliferation index when compared with patient-derived tissues (29) due to the requirement to add exogenous growth factors to maintain tissue viability (30). Most mortal engineered epithelia had a very low proliferative index, likely reflecting the inherent tendency of these cells to differentiate and eliminate abnormal cells from the epithelium *in vivo* and our inability to define growth conditions that could support continued proliferation of these cells. However, in all other respects, these engineered dysplastic epithelia resemble the clinical lesions remarkably closely and, together with the normal counterparts, provide a new resource for assessing the efficacy of novel approaches for the treatment of oral precancer.

We anticipated that the grade of the dysplasia would be the most important factor influencing lysis, but this was not the only parameter modulating the lytic effect, and we examined other tissue characteristics that we considered might affect the response to *dl*922-947. Replication of CRAds occurs in cycling cells, and we anticipated that we might see lysis of the basal layer of engineered normal oral epithelia, but few lytic foci were observed. The proliferation index for the basal and suprabasal compartments of most mortal engineered dysplastic epithelia was low, although the strain with the most cycling basal cells showed a high lysis score after exposure to 100 vp per cell. We also found that increasing the number of suprabasal cycling cells, by maintaining the D20

dysplastic epithelia with EGF as opposed to KGF, increased the lytic effect. However, the POE9n epithelia, with a high basal proliferation index, showed only patchy basal cell lysis following infection with *dl*922-947, indicating that whereas the number of replicating cells is important, other factors influence the treatment response.

Expression of key proteins influencing senescence and the G_1-S checkpoint (31–33) might also be important as keratinocytes lacking p16 and those with high levels of RbP cycle more frequently, and this may support more efficient replication and lysis. However, the engineered mortal dysplasias that expressed p16, low levels of pRbP, and wild-type p53 showed complete lysis after exposure to *dl*922-947 or Δ24. This suggests that the lytic effect of these CRAds may not necessarily be dependent of the loss of these critical regulatory proteins or *p53* gene status.

The finding that the mortal dysplastic epithelia lysed as efficiently as their immortal counterparts prompted us to investigate expression of p300, a cofactor that interacts with E1A to induce S phase (34). We anticipated that expression of p300 would be associated with differentiation (35), but this cofactor was widely expressed in normal and dysplastic epithelia, including those with a relatively undifferentiated phenotype.

Based on these observations, we propose that nonkeratinized normal oral mucosa resists lysis with *dl*922-947 because the multilayered nature of the epithelium, with abundant tight junctions, prevents any virus reaching the proliferative basal cells. When the epithelium is keratinized, the superficial layers provide an additional barrier, but if CRAds reach the spinous layers, replication might occur in cycling cells, or retention of the CR1 region in *dl*922-947 may stimulate S phase in postmitotic cells (36) producing focal lysis, and this effect was confirmed using our *in vitro* systems.

The engineered dysplasias express CAR on a proportion of the upper cell layers, and exposure of dysplastic keratinocytes to

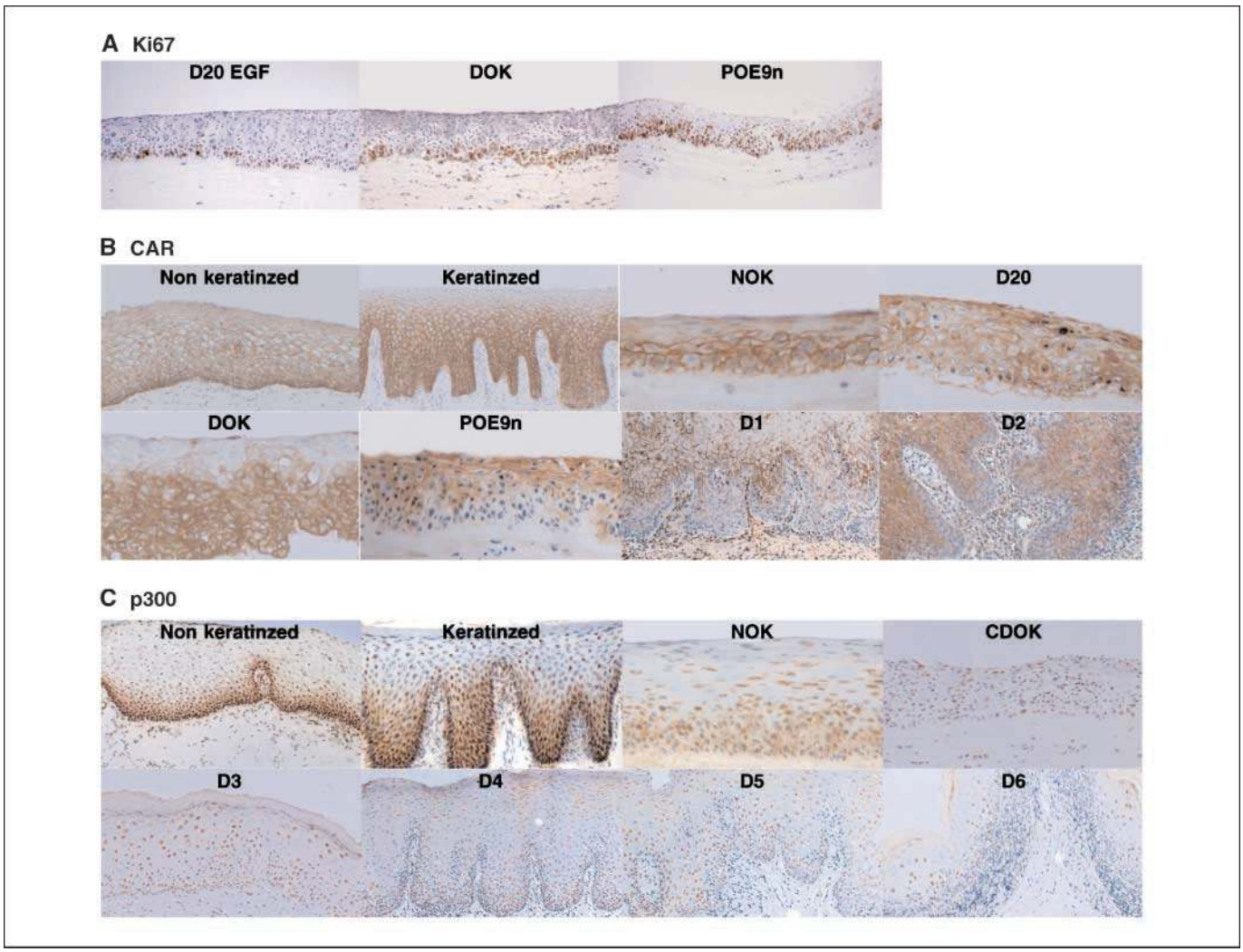

Figure 5. Demonstration of the tissue characteristics that modulate the lytic response. Representative examples of (*A*) Ki67 staining show a predominantly basal pattern for the tissue-engineered D20 epithelia maintained with KGF and DOK, whereas the POE9n epithelia had many suprabasal proliferating cells. *B,* the CAR was expressed throughout the epithelia for nonkeratinized buccal mucosa but restricted to the lower layers at keratinized sites. The typical pattern was recapitulated for tissue-engineered normal and dysplastic oral epithelia prepared using the D20, DOK, and POE9n strains. The engineered DOK dysplastic epithelia showed weak expression on the upper epithelial layers and the POE9n strain sites where this receptor was absent on the basal cells, a pattern that was also found for some clinical dysplastic lesions (*D1, D2*). *C,* expression of the cofactor p300 was restricted to the basal layer at nonkeratinized sites, but found throughout the epithelial layers for keratinized normal oral epithelia, the matched parakeratinzed tissue-engineered normal oral epithelium, and the CDOK mortal dysplastic epithelium. Most clinical dysplastic lesions expressed p300 throughout the epithelia (*D3–D5*), although some tissues (for example, *D6*) showed a mixed pattern with adjacent positive and negative areas.

*dl*922-947 increased the proportion of cells in S phase as previously reported (37), but this response was not seen when normal keratinocytes were exposed to this CRAd. Thus, we hypothesize that following the infection of dysplastic keratinocytes with *dl*922-947, S phase induction occurs due to the retention of the CR1 region, expression of p300, or aberrations affecting the cell cycle or apoptosis that promote viral replication, and that these effects contribute to the superior potency of *dl*922-947 when compared with Adwt. The high proliferation index and frequent suprabasal mitoses that characterize the immortal dysplasias, activation of adenovirus early promoters as differentiation occurs (E1A, E2A, and E4; ref. 38), together with the altered mechanisms for RNA export that promote viral replication (39), may also facilitate productive viral DNA amplification.

The location of E1A staining suggested that replication commenced at the sites where CAR is abundant and the progeny released following cell rupture enter adjacent cells using this receptor. The increased permeability of dysplastic epithelia compared with normal mucosa (40), or changes in cell shape and adhesion that occur during infection, may also help the virus to pass into the deeper tissues by a combination of repeat cycles of infection and replication. The virus may also infect oral keratinocytes via alternate primary receptors including perlecan (41) and the α2 domain of the MHC (42). We found that some dysplastic epithelia do not express CAR on the basal cells, and this may explain why lysis of the POE9n epithelia is largely confined to the upper layers. Low levels of E1A were detected in the basal keratinocytes that remained, strongly suggesting that if left for longer periods of time, complete lysis might occur.

We investigated whether Δ24RGD or Ad5/3Δ24, vectors that overcome any CAR deficiency (43–45), could lyse engineered dysplastic epithelia more efficiently, but found that these CRAds produced less lysis than *dl*922-947 or Δ24. The most likely explanations for this are that levels of Ad3 receptors are not as high on oral dysplasia as found for squamous tumors (13), and that intergrin expression is not sufficient to promote targeting and internalization of Δ24RGD. We found that some tissue-engineered dysplastic epithelia showed complete lysis after exposure to a single dose of *dl*922-947, whereas foci of basal cells remained when the POE9n and the SPDOK and LTDOK strains of mortal oral keratinocytes were exposed to this CRAd. It is to be anticipated that similar partial therapeutic effects would be seen in the clinic, but that repeat treatment with the same vector and developing protocols incorporating CRAds that infect cells using alternative primary receptors will help to maximize destruction of these abnormal keratinocytes. Ongoing improvements in vecterology that enhance the infectivity of these viruses (46–50) and exploit differences between normal and dysplastic oral keratinocytes, for example, increased expression of cell surface extracellular matrix components to further augment this process, may also be beneficial. However, effective destruction of all dysplastic keratinocytes will probably depend on developing strategies that exploit the knowledge of the pathways that sustain the suprabasal and increased proliferation of these clones, and the effect of combining the lytic effect of CRAds with small molecules that modulate epithelial proliferation can be tested in future studies.

Many patients prefer to have a precursor lesion removed to reduce the requirement for long-term follow-up to reduce the anxiety about the diagnosis and risk of tumor development. We have shown that *dl*922-947 has the potential to dissolve these lesions. This treatment may also be able to eliminate oral mucosa that looks normal on visual inspection, but is genetically and phenotypically abnormal, adding a degree of biological selectivity to the management of oral dysplasia.

Acknowledgments

Received 10/16/2006; revised 4/23/2007; accepted 5/23/2007.

The costs of publication of this article were defrayed in part by the payment of page charges. This article must therefore be hereby marked *advertisement* in accordance with 18 U.S.C. Section 1734 solely to indicate this fact.

We thank Dr. John Harrison for help with evaluating the morphology of these cultures and Dr. Kate Rauen for the kind gift of the CAR 72 antibody.

References

1. Califano J, van der Riet P, Westra W, et al. Genetic progression model for head and neck cancer: implications for field cancerization. Cancer Res 1996;56:2488–92.
2. Partridge M, Emilion G, Pateromichelakis S, Phillips E, Langdon J. Field cancerization of the oral cavity: comparison of the spectrum of molecular alterations in cases presenting with both dysplastic and malignant lesions. Oral Oncol 1997;33:332–7.
3. Partridge M, Pateromichelakis S, Phillips E, Emilion GG, A'Hern RP, Langdon JD. Allelic imbalance at chromosomal loci implicated in the pathogenesis of oral precancer, cumulative loss and its relationship with progression to cancer. Oral Oncol 1998;34:77–83.
4. Partridge M, Pateromichelakis S, Phillips E, et al. A case-control study confirms that microsatellite assay can identify patients at risk of developing oral squamous cell carcinoma within a field of cancerization. Cancer Res 2000;60:3893–8.
5. van Houten VM, Leemans CR, Kummer JA, et al. Molecular diagnosis of surgical margins and local recurrence in head and neck cancer patients: a prospective study. Clin Cancer Res 2004;10:3614–20.
6. Heise C, Hermiston T, Johnson L, et al. An adenovirus E1A mutant that demonstrates potent and selective systemic anti-tumoural efficacy. Nat Med 2000;6:1134–9.
7. Fueyo J, Gomes-Manzano C, Alemany R, et al. A mutant oncolytic adenovirus targeting the Rb pathway produces anti-glioma effect *in vivo*. Oncogene 2000;19:2–12.
8. Li D, Duan L, Freimuth P, O'Malley BW. Variability of adenovirus receptor density influences gene transfer efficacy and therapeutic response in head and neck cancer. Clin Cancer Res 1999;5:4175–81.
9. Douglas JT, Kim M, Sumerel LA, Carey DE, Curiel DT. Efficient oncolysis by a replicating adenovirus (Ad) *in vivo* is critically dependent on tumor expression of primary Ad receptors. Cancer Res 2001;61:813–7.
10. Hamidi S, Salo T, Kainulainen T, et al. Expression of α(v)β6 integrin in oral leukoplakia. B J Cancer 2000;82:1433–40.
11. Regezi JA, Ramos DM, Pytela R, Dakker NP, Jordan RC. Tenascin and β6 integrin are overexpressed in floor of the mouth *in situ* carcinomas. Oral Oncol 2002;38:332–6.
12. Suzuki K, Fueyo J, Krasnykh V, Reynolds PN, Curiel DT, Alemany R. A conditionally replicative adenovirus with enhanced infectivity shows improved oncolytic potency. Clin Cancer Res 2001;7:120–6.
13. Kawakami Y, Li H, Lam JT, Krasnykh V, Curiel DT, Blackwell JL. Substitution of the adenovirus serotype 5 knob with a serotype 3 knob enhances multiple steps in virus replication. Cancer Res 2003;63:1262–9.
14. Sirena D, Lilienfeld B, Eisenhut M, et al. The human membrane cofactor CD46 is a receptor for species B adenovirus serotype 3. J Virol 2004;78:4454–62.
15. Short JJ, Pereboev AV, Kawakami Y, et al. Adenovirus serotype 3 utilizes CD80 (B7.1) and CD86 (B7.2) as cellular attachment receptors. Virology 2004;322:349–59.
16. Heise C, Sampson-Johannes A, Williams A, et al. ONYX-015, an EI B gene-attenuated adenovirus, causes tumor-specific cytolysis and antitumoral efficacy that can be augmented by standard chemotherapeutic agents. Nat Med 1997;3:639–45.
17. McCormick F. ONYX-015 selectivity and the p14ARF pathway. Oncogene 2000;19:6670–2.
18. Reis SJ, Brandts CH, Chung AS, et al. Loss of p14ARF in tumour cells facilitates replication of the adenovirus mutant dl1520 (ONYX-015). Nat Med 2000;6:1128–33.
19. Rudin CM, Cohen EE, Papadimitrakopoulou VA, et al. An attenuated adenovirus, ONYX-015, as mouthwash therapy for premalignant oral dysplasia. J Clin Oncol 2003;21:4546–52.
20. Wang Y, Thorne S, Hannock J, et al. A novel assay to assess primary human cancer infectibility by replication-selective oncolytic adenoviruses. Clin Cancer Res 2005;11:351–60.
21. Partridge M, Green MR, Langdon JD, Feldmann M. Production of TGF-α and TGF-β by cultured keratinocytes, skin and oral squamous cell carcinomas—potential autocrine regulation of normal and

malignant epithelial cell proliferation. Br J Cancer 1989;60:542–8.
22. McGregor F, Muntoni A, Fleming J, et al. Molecular changes associated with oral dysplasia progression and acquisition of immortality: potential for its reversal by 5-azacytidine. Cancer Res 2002;62:4757–66.
23. Chang SE, Foster S, Betts D, et al. DOK, a cell line established from human dysplastic oral mucosa, shows a partially transformed non-malignant phenotype. Int J Cancer 1992;52:896–902.
24. Dickson MA, Hahn WC, Ino Y, et al. Human keratinocytes that express hTERT and also bypass a p16 (INK4a)-enforced mechanism that limits life span become immortal yet retain normal growth and differentiation characteristics. Mol Cell Biol 2000;20:1436–47.
25. Easty DM, Easty GC, Carter RL, Monaghan P, Butler LJ. Ten human carcinoma cell lines derived from squamous carcinomas of the head and neck. Br J Cancer 1981;43:772–85.
26. Igarashi M, Irwin CR, Locke M. Mackenzie IC. Construction of large area organotypical cultures of oral mucosa and skin. J Oral Pathol Med 2003;32:422–30.
27. Rauen KA, Sudilovsky D, Le JL, et al. Expression of the coxsackie adenovirus receptor in normal prostate and in primary and metastatic prostate carcinoma: potential relevance to gene therapy. Cancer Res 2002;62:3812–8.
28. Partridge M, Smith CG, Green MR. Differences between the distribution of epidermal growth factor receptor in human skin and oral mucosa, detected by immunohistology and EGF binding studies. Epithelia 1988;1:179–90.
29. Thompson PJ, Soames JV, Booth C, O'Shea JA. Epithelial cell proliferative activity and oral cancer progression. Cell Prolif 2002;35:110–20.
30. Stark H-J, Wilhauck MJ, Mirancea N, et al. Authentic fibroblast matrix in dermal equivalents normalises epidermal histogenesis and dermo-epidermal junction in organotypic co-culture. Eur J Cell Biol 2004;83:631–45.
31. Papadimitrakopoulou V, Izzo J, Lippman SMG, et al. Frequent inactivation of p16INK4a in oral premalignant lesions. Oncogene 1997;14:1799–803.
32. Shintani S, Mihara M, Nakahara Y, et al. Expression of cell cycle control proteins in normal epithelium, premalignant and malignant lesions of oral cavity. Oral Oncol 2002;38:235–43.
33. Oliver RJ, MacDonald DG. G_1 cyclins in oral epithelial dysplasia. J Oral Pathol Med 2001;30:80–6.
34. Howe JA, Bayley ST. Effects of AdE1A mutant viruses on the cell cycle in relation to the binding of cellular proteins including the retinoblastoma protein and cyclin A. Virology 1992;196:15–24.
35. Goodman RH, Smolik S. CBP/p300 in cell growth, transformation and development. Genes Dev 2000;14:1553–77.
36. Berk AJ. Lessons in gene expression, cell cycle control, and cell biology from adenovirus. Oncogene 2005;24:7673–85.
37. Lockley M, Fernandez M, Wang Y. Activity of the adenoviral E1A deletion mutant dl922-947 in ovarian cancer: comparison with E1A wild type viruses, bioluminescence monitoring and intraperitoneal delivery in icodextrin. Cancer Res 2005;6:989–98.
38. Noya F, Balague C, Banerjee NS, Curiel DT, Broker TR, Chow LT. Activation of adenovirus early promoters and lytic phase in differentiated strata of organotypic cultures of human keratinocytes. J Virol 2003;77:6533–40.
39. O'Shea CC, Johnson L, Bague B, et al. Late viral RNA export, rather than p53 inactivation, determines ONYX-O15 tumour selectivity. Cancer Cell 2004;6:611–23.
40. Banoczy J, Squier CA, Kremer M, et al. The permeability of oral leukoplakia. Eur J Oral Sci 2003;111:312–5.
41. Ikarashi T, Yonemochi H, Ohshiro K, Cheng J, Saku T. Intraepithelial expression of perlecan, a basement membrane-type heparan sulphate proteoglycan reflects dysplastic changes of the oral mucosal epithelium. J Oral Pathol Med 2004;33:87–95.
42. Prime SS, Pitigala-Arachchi A, Crane IJ. The expression of cell surface MHC class I heavy and light chain molecules in pre-malignant and malignant lesions of the oral mucosa. Histopathology 1987;11:81–91.
43. Stenenson SC, Rollence M, Marshall-Neff J, McClelland A. Selective targeting of human cells by a chimeric adenovirus vector containing a modified fiber protein. J Virol 1997;71:2782–90.
44. Wu H, Seki T, Dmitriev I, et al. Double modification of adenovirus fiber with RGD and polylysine motifs improves coxsackievirus-adenovirus receptor-independent gene transfer efficiency. Hum Gene Ther 2002;13:1647–53.
45. Kaneva A, Zinn KR, Chaudhuri TR, et al. Enhanced therapeutic efficacy for ovarian cancer with serotype 3 receptor-targeted oncolytic adenovirus. Mol Ther 2003;8:1–10.
46. Krasnykh V, Belousova N, Korokhov N, Mikheeva G, Curiel DT. Genetic targeting of an adenoviral vector via replacement of the fibre protein with the phage T4 fibritin. J Virol 2001;75:4176–83.
47. Belousova N, Krendelchtchikova V, Curiel DT, Krasnykh V. Modulation of adenovirus vector tropism via incorporation of polypeptide ligands into the fibre protein. J Virol 2003;76:8621–31.
48. Borovjagin AV, Krendelchtchikov A, Ramesh N, Yu D-C, Douglas JT, Curiel DT. Complex mosaicism is a novel approach to infectivity enhancement of adenovirus type 5-based vectors. Cancer Gene Ther 2005;12:475–86.
49. Stoff A, Rivera AA, Banerjee NS, et al. Strategies to enhance transduction efficiency of adenoviral-based gene transfer to primary human fibroblasts and keratinocytes as a platform in dermal wounds. Wound Repair Regen 2006;14:608–17.
50. Tyler MA, Ulasov IV, Borovjagin A, et al. Enhanced transduction of malignant glioma with a double targeted Ad5/3-RGD fibre-modified adenovirus. Mol Cancer Ther 2006;5:2408–16.

Lysis of Dysplastic but not Normal Oral Keratinocytes and Tissue-Engineered Epithelia with Conditionally Replicating Adenoviruses

Kamis Gaballah, Allison Hills, David Curiel, et al.

Cancer Res 2007;67:7284-7294.